

## Ultrahigh-resolution (1+1) photoionization spectroscopy of Kr I: Hyperfine structures, isotope shifts, and lifetimes for the $n = 5, 6, 7$ $4p^5ns$ Rydberg levels

T. Trickl,\* M. J. J. Vrakking, E. Cromwell, Y. T. Lee, and A. H. Kung

*Materials and Chemical Sciences Division, Lawrence Berkeley Laboratory and Department of Chemistry,  
University of California at Berkeley, Berkeley, California 94720*

(Received 8 August 1988)

High-resolution measurements of the hyperfine structures and isotope shifts are reported for Kr I  $n = 5, 6, 7$   $4p^5ns$  Rydberg levels, obtained using an extreme-ultraviolet laser with a bandwidth of 210 MHz in a resonant two-photon-ionization scheme. Use of known  $I_2$  frequencies yields an improved absolute calibration of the Kr energy levels by more than one order of magnitude. The nuclear quadrupole hyperfine structure indicates that the  $4p^56s$  and  $4p^57s$  states are described by a pure  $jj$ -coupling scheme, whereas the  $4p^55s$  states depart from a pure  $jj$ -coupling scheme by 0.37(6)%. The magnetic hyperfine structure shows that the  $4p^5ns$  states are mixed with  $4p^5n'd$  states. The isotope shifts can be described as pure mass effects within the precision of our experiment. For the  $4p^56s$  and  $4p^57s$  states, lifetimes were determined that differ markedly from theoretical literature values.

### I. INTRODUCTION

The spectroscopy of krypton has been studied previously in very high resolution by interferometric methods, by magnetic resonance, and by laser spectroscopy.<sup>1-25</sup> The 605.78-nm line of  $^{86}\text{Kr}$  was chosen as the primary wavelength standard.<sup>26</sup> The element has six stable isotopes:  $^{78}\text{Kr}$  (0.35% natural abundance),  $^{80}\text{Kr}$  (2.27%),  $^{82}\text{Kr}$  (11.56%),  $^{83}\text{Kr}$  (11.55%),  $^{84}\text{Kr}$  (56.90%), and  $^{86}\text{Kr}$  (17.37%).<sup>27</sup> Among these, only  $^{83}\text{Kr}$  has a nonzero nuclear angular momentum  $I = \frac{9}{2}$ . Various visible and near-infrared transitions of these isotopes and the hyperfine structure of the metastable  $5s [^2P_{3/2}] J = 1$  state of  $^{83}\text{Kr}$  have been evaluated.<sup>5,6,12,13,17,22,23,25</sup> For these transitions the Kr isotope shifts are rather small,<sup>10-16,23</sup> typically smaller than  $0.005 \text{ cm}^{-1}$ . Therefore, very careful measurements by interferometry or laser spectroscopy are necessary to determine the shifts and to determine the contribution of the nuclear mass and in particular the much smaller effect of the nuclear volume to these shifts. Some irregularities of the nuclear volume effect were found.<sup>10,11,15,19,23</sup>

All the accurate measurements mentioned above used transitions between the excited states, frequently starting from metastable states which can be populated in measurable quantities in a discharge. This was necessary because transitions to the ground state of Kr are in the vacuum ultraviolet region of the spectrum where high-resolution sources were not available. Selection rules excluded the precise study of many states optically connected to the ground state. Furthermore, the absolute frequency of the Kr transitions relative to the ground state is only known to within  $\pm 0.15 \text{ cm}^{-1}$ .<sup>7,28</sup> Hence, in order to complete the mapping of the spectroscopy of Kr it is essential to obtain precise spectroscopic information with regard to the ground state of Kr.

Recently, we have developed an ultrahigh-resolution photoionization spectrometer, consisting of a single-frequency broadly tunable vacuum-ultraviolet-extreme-ultraviolet (vuv-xuv) laser source<sup>29</sup> and a pulsed molecu-

lar beam apparatus. The source provides continuously tunable radiation from 74 nm to the visible region with a spectral resolution of smaller than 210 MHz and a photon flux exceeding  $10^{10}$  per pulse at 10 Hz. This makes possible for the first time the study of high-resolution spectroscopy and dynamics of atoms and molecules in the vuv-xuv region.

In this paper hyperfine splittings, isotope shifts, and lifetimes of a series of Kr  $4p^5ns$  states are reported. These results are obtained by direct excitation from the ground state, in a wavelength range between 94.5 nm and 123.6 nm. The nuclear quadrupole hyperfine splitting is interpreted in terms of a change of the coupling between the atomic core and the orbital electron, as a function of the principle quantum number of the latter. It is found that the  $4p^56s$  and  $4p^57s$  configurations can be described in a pure  $jj$ -coupling scheme, whereas the  $4p^55s$  configuration shows a slight departure from  $jj$  coupling. The magnetic hyperfine structure is analyzed in terms of individual contributions from the core-hole and the orbital electron. An application of  $jj$ -coupling models shows that there must be some mixing of the  $4p^5ns$  configurations with nearby  $4p^5n'd$  configurations. In studying the isotope shifts, our measurements reveal no conclusive departure from a pure mass effect. Therefore contributions from the volume effect must fall within the error limits of our experiment. The lifetimes of the  $4p^56s$  and  $4p^57s$  states were determined experimentally for the first time. They differ markedly from results of theoretical calculations. The photoionization spectra were calibrated by the  $I_2$  wavelength standard and yield absolute frequencies for the krypton level manifold, which are approximately 20 times more precise than before.

### II. EXPERIMENT

The narrow-band pulsed dye laser system is described in a separate publication.<sup>29</sup> Briefly, a cw dye laser (Coherent Radiation CR 699-29 Autoscan) is pulse amplified in four amplification stages. The amplifier dye

cells are side pumped by the second harmonic output of a single-longitudinal-mode Nd-YAG laser (Quantel YG 592 with injection seeding). Typical output powers in the wavelength region between 564 and 616 nm are 60 to 120 mJ/pulse. The bandwidth measured is about 95 MHz. Frequency doubling yields uv pulse energies of up to 40 mJ/pulse. Vacuum ultraviolet (vuv) light is generated by four-wave frequency mixing in a pulsed jet. Table I lists the states of krypton that were investigated, as well as the amplifier dyes, vuv generation schemes, and mixing gasses used.

The vuv light is separated from the more powerful uv light in a 1-m vacuum monochromator (McPherson, model 225) in order to avoid power broadening and ac Stark shifts. The curved monochromator grating re-focusses the laser beam into the photoionization chamber where the laser beam intersects a pulse krypton beam 16 cm from the nozzle with a photon beam diameter of about 5 mm or less, as determined by an aperture in the uv beam. The pulsed atomic beam source is differentially pumped and operates with a nozzle-skimmer distance of 100 mm and a skimmer diameter of 1.0 mm, resulting in a relative Doppler width  $\delta\nu/\nu = 1.0 \times 10^{-8}$ . The krypton backing pressure behind the 0.2-mm-wide nozzle was adjusted to minimize line distortions due to saturation broadening. For the strongest transitions the absorption was found to be near 100% at an atomic beam diameter of roughly 1.5 mm for backing pressures  $\geq 1$  bar.

The excited atoms were photoionized with a second laser (Quanta-Ray DCR-2A or PDL). The wavelengths used for this laser are given in Table I. When probing states with lifetimes long compared to the laser pulsewidth the second laser was delayed with respect to the vuv pulse. The second laser was attenuated to approximately 0.5 mJ/pulse when short lifetimes of the excited atoms made temporal overlapping of the first and second laser pulses necessary. Under this condition no power broadening was observed. The minimum linewidth observed was  $0.007 \text{ cm}^{-1}$  (210 MHz) full width half maximum.

The different isotopes were separated using a time-of-flight mass spectrometer. Spectra for pairs of isotopes were measured simultaneously by setting two boxcar

gates to selected mass peaks. The mass resolution could be improved by reducing the diameter of the first laser beam with an aperture, though the ion signal was then reduced to a rather low level. Thus many of the spectra show fluctuations. Accurate line positions were obtained by averaging over several scans.

Hyperfine structure scans of  $^{83}\text{Kr}$  were mostly recorded using a quadrupole mass filter. This was necessary to suppress contributions from stronger lines of more abundant neighboring isotopes.

The dc Stark shift due to the ion extraction field strength was examined and found to be about 70 MHz in the vuv for the  $7s[{}^2P_{3/2}] J=1$  state at about 100 V/cm and less for the other states. Therefore the dc Stark effect was negligible in the calibration scans, which were performed at extraction fields  $\leq 25$  V/cm.

Rough wavelength measurements were done by using the Autoscan wavemeter, which has a resettability of  $0.003 \text{ cm}^{-1}$ . A more refined calibration was achieved by an interpolation of the fringes of a 300-MHz reference étalon. The slight drift of the free spectral range of this étalon was corrected using  $I_2$  absorption spectra, which were recorded simultaneously.

### III. RESULTS AND DISCUSSION

Tables II–V summarize the results for the absolute calibrations, hyperfine parameters, isotope shifts, and excited-state lifetimes for the  $4p\ ^6(1S_0) \rightarrow 5s'[{}^2P_{1/2}] J=1$ ,  $6s'[{}^2P_{1/2}] J=1$ ,  $5s[{}^2P_{3/2}] J=1$ ,  $6s[{}^2P_{3/2}] J=1$ ,  $7s[{}^2P_{3/2}] J=1$  transitions. The typical accuracy of the measurements of relative Kr line positions with the continuous laser is 2 MHz in the visible for small differences and 3 MHz for the largest hyperfine intervals. Typical experimental results are given in Figs. 1 and 3, which show the  $^{83}\text{Kr}$  hyperfine structures for all transitions measured and the isotope shifts for the  $4p\ ^6(1S_0) \rightarrow 4p\ ^57s[{}^2P_{3/2}] J=1$  transition, respectively.

#### A. Absolute calibrations of $^{86}\text{Kr}$ line positions

A large number of very precise interferometric measurements have been reported for transitions between ex-

TABLE I. Summary of experimental conditions (see text).

State	$\nu(^{86}\text{Kr})$ ( $\text{cm}^{-1}$ ) <sup>a</sup>	$\nu_{\text{visible}}$ ( $\text{cm}^{-1}$ )	Amplifier dye	vuv generation	Mixing gas	Wavelength ionizing laser (nm)
$5s[{}^2P_{3/2}] J=1$	80 916.757	17 578.4	Rh 590	$3 \times (9394 \text{ cm}^{-1} + \nu_{\text{visible}})^b$	CO	266
$5s'[{}^2P_{1/2}] J=1$	85 846.694	17 169.3389	basic Rh 610	$2 \times 2\nu_{\text{visible}} + \nu_{\text{visible}}$	Xe	355
$6s[{}^2P_{3/2}] J=1$	99 894.040	16 649.0067	Rh 640	$3 \times 2\nu_{\text{visible}}$	Ar	266
$6s'[{}^2P_{1/2}] J=1$	105 146.294	17 524.3823	Rh 590	$3 \times 2\nu_{\text{visible}}$	Xe	560
$7s[{}^2P_{3/2}] J=1$	105 770.695	17 628.4492	Rh 590	$3 \times 2\nu_{\text{visible}}$	Xe	560

<sup>a</sup>This column corresponds to the energy given in Ref. 7, corrected by  $-0.0679 \text{ cm}^{-1}$ , as recommended in Sec. III of the present paper.

<sup>b</sup>Approximate Nd-YAG laser frequency.

TABLE II. Absolute calibration of  $^{86}\text{Kr}$ . Comparison of absolute frequencies from  $I_2$  calibrations to literature values.

State	$\nu$ (cm $^{-1}$ )	$\nu$ (Ref. 32) (cm $^{-1}$ )	$\Delta\nu$ (Ref. 32) (cm $^{-1}$ )	$\nu$ (Ref. 7) (cm $^{-1}$ )	$\Delta\nu$ (Ref. 7) (cm $^{-1}$ )
$5s'[^2P_{1/2}] J=1$	85 846.7000(79)	85 847.501	0.8010	85 846.7624	0.0624
$6s'[^2P_{1/2}] J=1$	105 146.3095(138)	105 147.13	0.8205		
$6s[^2P_{3/2}] J=1$	99 894.0337(73)	99 894.83	0.7963	99 894.1081	0.0744
$7s[^2P_{3/2}] J=1$	105 770.6962(73)	105 771.50	0.8038	105 770.7632	0.0670

cited states of  $^{86}\text{Kr}$  because of the significance of  $^{86}\text{Kr}$  as a primary wavelength standard. Most of these measurements were reexamined and summarized by Kaufman and Humphreys.<sup>7</sup> Their table of excited-state frequencies has an internal coherence of  $10^{-4}$ – $10^{-3}$  cm $^{-1}$ . However, the absolute calibration is only given to within  $\pm 0.15$  cm $^{-1}$ , limited by the accuracy of vuv data by Petersson.<sup>28</sup>

Careful calibrations of our continuous-wave dye laser provide a considerably more precise determination of the absolute  $^{86}\text{Kr}$  level positions. The results are listed in column 1 of Table II (no calibration could be carried out for the  $5s'[^2P_{3/2}] J=1$  state, since the vuv generation in this experiment involved mixing with the Nd-YAG laser, the wavelength of which is not calibrated). The error analysis takes into account uncertainties in the center-of-gravity determination for the broad  $I_2$  absorption lines and “noise” of the wave numbers as given by Gerstenkorn and Luc,<sup>30</sup> as well as the absolute calibration error of the  $I_2$  atlas of  $\pm 0.0010$  cm $^{-1}$  after offset subtraction.<sup>31</sup> Furthermore, a +9-MHz shift of the pulse-amplified visible beam with respect to the cw ring dye laser and a small Doppler shift due to a 97.5° angle between the vuv beam and the atomic beam are corrected for. Two  $I_2$  lines next to the  $5s'[^2P_{1/2}] J=1$  and  $6s'[^2P_{1/2}] J=1$  frequencies, respectively, depart markedly from the  $\pm 0.0010$  cm $^{-1}$  error margin. For the  $6s'$  case this was confirmed by comparing the overlapping region of parts II and III of Ref. 30.

The corresponding Kr transition frequencies given by Moore<sup>32</sup> and by Kaufman and Humphreys<sup>7</sup> are included in Table II. The average offsets with respect to our data are 0.805(11) and 0.0679(61) cm $^{-1}$ , respectively. The small standard deviations of these averages are indicative of the accuracy of our evaluation. It is therefore recommended to subtract 0.0679(61) cm $^{-1}$  from the energy values in Table II of Ref. 7 to obtain an improved set of vuv reference lines between 80 000 and 110 000 cm $^{-1}$ .

## B. $^{83}\text{Kr}$ hyperfine structure

A selection of scans of the  $^{83}\text{Kr}$  hyperfine structure is shown in Fig. 1. The hyperfine structure contains contributions from the magnetic interaction between the nuclear magnetic moment  $\mu_I$  and the magnetic field at the nucleus produced by orbital electrons ( $A$  parameter), as well as from the electrostatic interaction between the nuclear quadrupole moment and the gradient of the electric field at the nucleus produced by orbital electrons ( $B$  parameter). The hyperfine energies of the multiplet are given by<sup>33</sup>

$$W = A \frac{C}{2} + B \frac{\frac{3}{4}C(C+1) - I(I+1)J(J+1)}{2I(I-1)J(2J-1)}, \quad (1)$$

with  $C = F(F+1) - I(I+1) - J(J+1)$ .

The  $A$  and  $B$  parameters derived from a least-squares fit of the hyperfine splittings observed in the present experiments are summarized in Table III along with the only two pairs of literature values available for comparison.

### 1. $B$ parameters

When an electron is promoted out of a  $4p^6$  Kr ground-state configuration to a  $ns$  orbital, there are two possible  $J=1$  states which can be occupied, designated by  $^3P_1$  and  $^1P_1$ . The wave functions of these states can be expressed as a superposition of wave functions corresponding to either a  $^2P_{j=3/2}$  or  $^2P_{j=1/2}$  core,

$$\begin{aligned} \Psi(^3P_1) = & \cos(\delta)\Psi(j_p = \frac{3}{2}, j_s = \frac{1}{2}) \\ & + \sin(\delta)\Psi(j_p = \frac{1}{2}, j_s = \frac{1}{2}), \end{aligned} \quad (2a)$$

$$\begin{aligned} \Psi(^1P_1) = & -\sin(\delta)\Psi(j_p = \frac{3}{2}, j_s = \frac{1}{2}) \\ & + \cos(\delta)\Psi(j_p = \frac{1}{2}, j_s = \frac{1}{2}), \end{aligned} \quad (2b)$$

where  $j_p$  and  $j_s$  represent the angular momenta of the  $4p^5$

TABLE III. Hyperfine parameters for  $^{83}\text{Kr}$ 

State	$A$ (cm $^{-1}$ )	$B$ (cm $^{-1}$ )	$A$ (Ref. 12) (cm $^{-1}$ )	$B$ (Ref. 12) (cm $^{-1}$ )
$5s'[^2P_{1/2}] J=1$	−0.024 678(55)	−0.003 87(32)	−0.024 67(1.5)	−0.003 72(10)
$6s'[^2P_{1/2}] J=1$	−0.017 405(96)	−0.000 23(55)		
$5s[^2P_{3/2}] J=1$	−0.005 357(63)	−0.003 69(28)	−0.005 35(2)	−0.003 53(10)
$6s[^2P_{3/2}] J=1$	−0.004 751(53)	−0.007 25(88)		
$7s[^2P_{3/2}] J=1$	−0.004 622(45)	−0.006 81(60)		

TABLE IV. Isotope shifts (all values in  $\text{cm}^{-1}$ ).

State	$\nu(78)-\nu(86)$	$\nu(80)-\nu(86)$	$\nu(82)-\nu(86)$	$\nu(83)-\nu(86)$	$\nu(84)-\nu(86)$	$^{83}\text{Kr}$ offset
$5s'[{}^2P_{1/2}] J=1$	-0.006 89	-0.005 26	-0.003 48	-0.004 34	-0.001 48	-0.001 74(20)
$6s'[{}^2P_{1/2}] J=1$	-0.023 37	-0.018 11	-0.011 83	-0.009 38	-0.005 61	-0.000 49(30)
$6s[{}^2P_{3/2}] J=1$	-0.017 24	-0.012 11	-0.008 31	-0.005 12	-0.004 43	+0.001 18(40)
$7s[{}^2P_{3/2}] J=1$	-0.023 04	-0.016 99	-0.011 36	-0.009 07	-0.005 52	-0.000 52(50)

core and the  $ns$  orbital electron, respectively. Similarly the wave functions of these states can be expressed as a superposition of wave functions corresponding to  $LS$  coupling as

$$\Psi({}^3P_1) = \cos(\epsilon)\Psi_{LS}({}^3P_1) + \sin(\epsilon)\Psi_{LS}({}^1P_1), \quad (3a)$$

$$\Psi({}^1P_1) = -\sin(\epsilon)\Psi_{LS}({}^3P_1) + \cos(\epsilon)\Psi_{LS}({}^1P_1). \quad (3b)$$

The relation between  $\delta$  and  $\epsilon$  is given by

$$\cos(\delta) = \left[ \frac{l}{2l+1} \right]^{1/2} \cos(\epsilon) - \left[ \frac{l+1}{2l+1} \right]^{1/2} \sin(\epsilon), \quad (4)$$

where  $l$  is the angular momentum of the core hole ( $l=1$ ). Since the Kr Rydberg states are expected to be very closely  $jj$  coupled, the  ${}^3P_1$  and  ${}^1P_1$  states are commonly referred to as  $j_p = \frac{3}{2}$  and  $j_p = \frac{1}{2}$  states, respectively.

From expressions for the  $B$  parameters in  $sp$  configurations, the following formulas can be derived for the  $B$  parameters in the  $4p^5ns({}^3P_1, {}^1P_1)$  states as a function of the  $B$  parameter in the  $4p^5ns({}^3P_2)$  state and the coupling coefficient  $c = \cos\delta$ :

$$B({}^3P_1) = \frac{1}{2}B({}^3P_2) \left[ c^2 - 4\sqrt{2} \left[ \frac{S}{R'} \right] c(1-c^2)^{1/2} \right], \quad (5a)$$

$$B({}^1P_1) = \frac{1}{2}B({}^3P_2) \left[ 1 - c^2 + 4\sqrt{2} \left[ \frac{S}{R'} \right] c(1-c^2)^{1/2} \right], \quad (5b)$$

where  $S$  and  $R'$  are relativistic corrections, which we take for nuclear charge  $Z_i \approx Z - 4 = 32$ .<sup>4,33</sup>

The gradient of the electric field at the nucleus caused by the orbital electrons is due to the  $4p$  hole in a  $4p^5ns$  configuration. If the charge distribution of the  $ns$  electron is perfectly spherically symmetric this electron should not contribute. As a consequence, one would expect that the quadrupole hyperfine structure does not depend on the principal quantum number  $n$ . Within experimental errors this can actually be observed in our experi-

TABLE V. Lifetimes of Kr Rydberg states (all values in nsec).

State	This paper	Ref. 39 (theor.)	Ref. 43 (theor.)
$6s[{}^2P_{3/2}] J=1$	$33 \pm 3$	17.7	2.6
$6s'[{}^2P_{1/2}] J=1$	$50 \pm 5$	12.3	19.8–24.8
$7s[{}^2P_{3/2}] J=1$	$117 \pm 12$	10.1	3.2–3.6

ments. By adding up Eqs. (5a) and (5b) it follows that our data imply values for  $B({}^3P_2)$  of  $-453(16)$  MHz ( $5s$ ) and  $-449(64)$  MHz ( $6s$ ), which are both in good agreement with the  $5s$  values of  $B({}^3P_2)$  of  $-452.1572(21)$  MHz determined from atomic-beam magnetic resonance experiments.<sup>6</sup> In absence of measurements of the  ${}^3P_2$  quantities for the  $6s$  and  $7s$  configurations, we assume for our evaluations that the  $5s$  value of  $B({}^3P_2)$  is valid for the other two states as well.

The  $B({}^3P_1)/B({}^3P_2)$  and  $B({}^1P_1)/B({}^3P_2)$  ratios following from our experiments are listed in column 1 of Table VI. The values of the coupling constants  $c$  which correspond to these ratios are shown in column 2. Excellent agreement is observed between the coupling constants derived from the  $B$  parameters of the  ${}^3P_1$  and  ${}^1P_1$  states, as

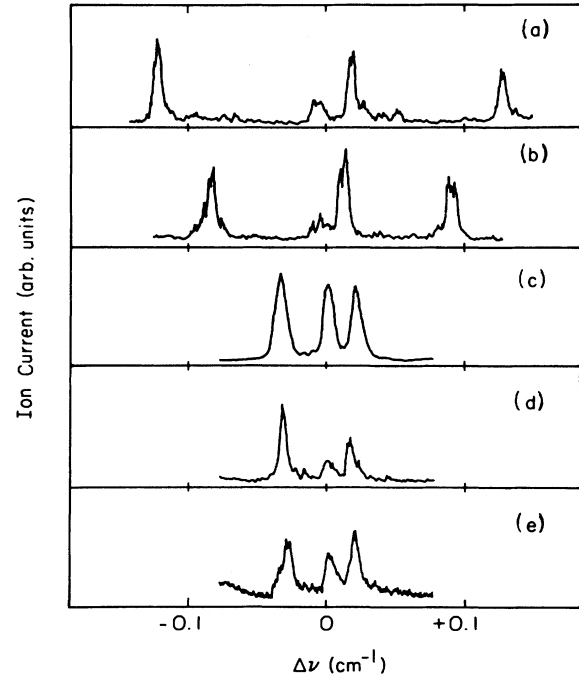


FIG. 1.  $^{83}\text{Kr}$  hyperfine structures observed for the transitions (a)  $4p^6({}^1S_0) \rightarrow 5s'[{}^2P_{1/2}] J=1$ , (b)  $6s'[{}^2P_{1/2}] J=1$ , (c)  $5s[{}^2P_{3/2}] J=1$ , (d)  $6s[{}^2P_{3/2}] J=1$ , and (e)  $7s[{}^2P_{3/2}] J=1$ . In all cases the three hyperfine components are from left to right  $F = \frac{11}{2}$ ,  $F = \frac{9}{2}$ ,  $F = \frac{7}{2}$  (splitting of upper state). The lines of spectrum C are wider because of the vuv generation scheme applied (see Table I). The extra smaller features on spectra A and B are due to neighboring mass ions leaking through the quadrupole mass filter. The horizontal scale is only relative.

TABLE VI. Coupling parameters for Kr  $4p^5ns$  configurations obtained from an analysis of the  $B$  parameters for the electric quadrupole hyperfine splitting.

State	$B/B(^3P_2)$	$c$	$c_{\text{average}}(n)$
$5s[{}^2P_{3/2}] J=1 (^3P_1)$	0.257(21)	0.996 21(57)	0.996 19(57)
$5s[{}^2P_{1/2}] J=1 (^1P_1)$	0.245(19)	0.996 17(57)	
$6s[{}^2P_{3/2}] J=1 (^3P_1)$	0.481(6)	$0.999\,978^{+0.000\,022}_{-0.000\,23}$	$0.999\,982^{+0.000\,018}_{-0.000\,20}$
$6s[{}^2P_{3/2}] J=1 (^1P_1)$	0.0153(365)	$0.999\,986^{+0.000\,014}_{-0.000\,18}$	
$7s[{}^2P_{3/2}] J=1 (^3P_1)$	0.451(4)	$0.999\,85^{+0.000\,15}_{-0.000\,30}$	$0.999\,85^{+0.000\,15}_{-0.000\,30}$

illustrated in Fig. 2. The observed  $B$  parameters can thus finally be understood by the observation that for the  $4p^56s$  and  $4p^57s$  configurations the  $J=1$  states can be described in a nearly pure  $jj$ -coupling scheme, whereas for the  $4p^55s$   $J=1$  configurations the nonunity coupling constant shows that there is some mixing of  $j_p = \frac{3}{2}$  and  $j_p = \frac{1}{2}$  configurations in the  ${}^3P_1$  and  ${}^1P_1$  states.

Our coupling parameter  $c$  for the  $4p^55s$  configurations differs from results obtained by other methods. Aydin reported a coupling coefficient obtained from the lifetimes of the  ${}^3P_1$  and the  ${}^1P_1$  states, after considering the spin-orbit interaction in first-order perturbation theory and diagonalizing the energy matrix.<sup>34</sup> His result  $\alpha = \sin(\epsilon) = -0.717$  corresponds to  $c = 0.9879$  [Eq. (4)]. This value is confirmed by values derived from  $g$  factors.<sup>24,35</sup> From Sears and McKellar's  $g({}^3P_1) = 1.2428(2)$  (Ref. 24) we calculate  $c = 0.988\,105(62)$  using the instructions of Ref. 34. Closer agreement with our coupling parameter  $c$  is obtained by using the improved lifetime data of Matthias *et al.*,<sup>36</sup> which give  $c = 0.9914$ .

## 2. $A$ parameters

The magnetic field at the nucleus produced by the orbital electrons contains contributions from both the  $4p$  hole and the  $ns$  orbital electron. Using the principle of energy sum rules, Goudsmit<sup>37</sup> has given expressions relat-

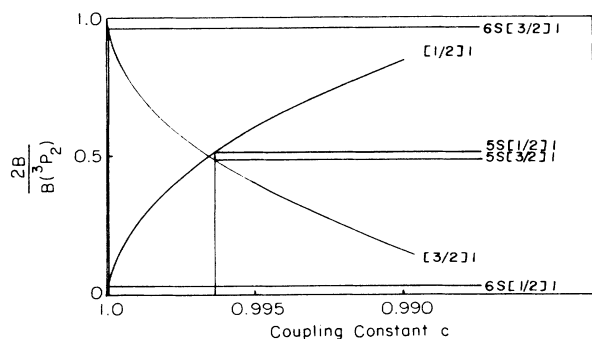


FIG. 2. Ratios  $2B(^3P_1)/B(^3P_2)$  and  $2B(^1P_1)/B(^3P_2)$  as a function of the coupling constant  $c$  [see Eqs. (5a) and (5b)]. Experimentally observed  $B(^3P_1)/B(^3P_2)$  and  $B(^1P_1)/B(^3P_2)$  ratios are used to determine the coupling constant  $c$  for the Kr  $n = 5, 6, 7$   $4p^5ns$  Rydberg levels. It is observed that the  $B$  parameter sensitively probes the transition from nearly pure ( $4p^55s$ ) to pure ( $4p^56s$  and  $4p^57s$ )  $jj$  coupling.

ing the  $A$  parameters for  $sp$  configurations in  $jj$  coupling to contributions from the  $s$  and  $p$  electrons. A more general treatment by Breit and Wills includes intermediate coupling and relativistic corrections.<sup>38</sup> For the  $4p^5ns$  case one has for  $j_s = \frac{1}{2}$ ,  $j_p = \frac{3}{2}$ , and  $J = 2$ ,

$$A(^3P_2) = \frac{1}{4}a_s + \frac{3}{4}a_{p,3/2}, \quad (6a)$$

for  $j_s = \frac{1}{2}$ ,  $j_p = \frac{3}{2}$ , and  $J = 1$

$$A(^3P_1) = \frac{2\sin^2(\delta) - \cos^2(\delta)}{4}a_s + \frac{5}{4}\cos^2(\delta)a_{p,3/2} + \frac{1}{2}\sin^2(\delta)a_{p,1/2} + \sqrt{2}\sin(\delta)\cos(\delta)a_p''', \quad (6b)$$

and for  $j_s = \frac{1}{2}$ ,  $j_p = \frac{1}{2}$ , and  $J = 1$ ,

$$A(^1P_1) = \frac{2\cos^2(\delta) - \sin^2(\delta)}{4}a_s + \frac{5}{4}\sin^2(\delta)a_{p,3/2} + \frac{1}{2}\cos^2(\delta)a_{p,1/2} - \sqrt{2}\sin(\delta)\cos(\delta)a_p''', \quad (6c)$$

where  $\cos(\delta)$  and  $\sin(\delta)$  are defined by Eqs. (2a) and (2b). For  $\delta=0$  Eqs. (6a), (6b), and (6c) agree with Goudsmit's expressions. The level assignments of the  ${}^3P_1$  and  ${}^1P_1$  states are opposite to the one by Breit and Wills<sup>38</sup> (see, e.g., Ref. 4). Equations (6a), (6b), and (6c) were derived under a one-electron approximation. This may lead to discrepancies for strongly perturbed levels. However, Breit and Wills state that for nearly pure  $jj$  coupling the experimental data are usually accurately described by the model.

The parameters  $a_{p,3/2}$ ,  $a_{p,1/2}$ , and  $a_p'''$  are interdependent. From the relations of Ref. 38 we get

$$a_{p,1/2} = 5 \frac{F_r(\frac{1}{2}, Z_i)}{F_r(\frac{3}{2}, Z_i)} a_{p,3/2}, \quad (7a)$$

TABLE VII. Magnetic hyperfine coefficients calculated from the  $A$  parameters assuming one-electron contributions. Numbers in parentheses represent error bars due to experimental uncertainties.

$a_{4p,1/2} = -0.036\,987(80) \text{ cm}^{-1}$
$a_{4p,3/2} = -0.006\,807(15) \text{ cm}^{-1}$
$a_p''' = 0.002\,132(5) \text{ cm}^{-1}$
$a_{5s} = -0.012\,132(44) \text{ cm}^{-1}$
$\cos(\delta)_{5s} = 0.996\,93(60)$
$a_{6s}({}^3P_1) = -0.014\,96(21) \text{ cm}^{-1a}$
$a_{6s}({}^1P_1) = -0.000\,644(4) \text{ cm}^{-1a}$
$a_{7s}({}^3P_1) = -0.015\,37(18) \text{ cm}^{-1a}$

<sup>a</sup>For the evaluation of these quantities we took the  $c = \cos(\delta)$  values from Table VI.

$$a_p''' = -\frac{5}{16} \frac{G_r(1, Z_i)}{F_r(\frac{3}{2}, Z_i)} a_{p,3/2}, \quad (7b)$$

where  $F_r$  and  $G_r$  are relativistic corrections listed by Kopfermann,<sup>33</sup> and  $Z_i \approx Z - 4 = 32$  for a Kr  $p$  hole.<sup>4,33</sup>

Following from these expressions the  $A$  parameters would essentially be due to four one-electron contributions, namely,  $a_{4p,3/2}$ ,  $a_{5s}$ ,  $a_{6s}$ , and  $a_{7s}$ , as well as the coefficient  $\cos(\delta)_{5s}$  which describes the intermediate coupling of the  $5s$  states. As we will point out later, the  $6s$  and  $7s$  states are in part mixed with  $4d$  and  $5d$  levels. Thus we derive  $a_{6s}$  and  $a_{7s}$  values for  $^3P_1$  and  $^1P_1$  separately as proposed by Breit and Wills for the case of large fine-structure splitting.<sup>38</sup> The results of our calculations are given in Table VII.

For the  $4p^55s$  configuration we observe excellent agreement of the theoretical model and our experimental data.  $a_{p,3/2}$  and  $a_{5s}$  are calculated from Eq. (6a) and the sum of Eqs. (6b) and (6c) taking  $A(^3P_2)$  from Ref. 6. A third quantity is evaluated from the difference of Eqs. (6b) and (6c). If we take  $[\cos(\delta)]_{5s} = 0.99619(57)$  from Table VI this procedure yields  $A(^3P_1) - A(^1P_1) = 0.019292 \text{ cm}^{-1}$  which is nearly identical with the experimental value of  $0.019321(83) \text{ cm}^{-1}$ . A calculation of  $\cos(\delta)$  from the experimental  $A(^3P_1) - A(^1P_1)$  yields a complex number for  $Z_i < 32.227$  ( $Z_i$  determined by interpolation of Kopfermann's tables<sup>33</sup>). For  $Z_i = 32.227$  we get  $[\cos(\delta)]_{5s} = 0.99693$  which is close to the value obtained from the  $B$  parameters. All coefficients of Table VII were calculated for  $Z_i = 32.227$ .

At this point, we do not see a simple explanation for the obvious discrepancies between the  $5s$  coupling coefficient derived from our  $A$  and  $B$  parameters and the ones from other work. There is little influence from experimental error on the value. We found that the most critical quantities of the model are the relativistic correction factors for the  $A$  parameter parametrization as a function of  $Z$ . However, this is clearly not the case for the  $B$  parameters.

The value of  $a_{6s}$  derived from the  $^3P_1$  state [Eq. (6b)] differs substantially from the one calculated for  $^1P_1$  [Eq. (6c)]. This difference is indicative of the presence of configuration mixing which was shown by Aymar and Coulombe in a parametric study of the Kr  $4p^5(5s+6s+7s+4d+5d+6d)$  levels.<sup>39</sup> Their results indicate that the  $4p^56s$  and  $4p^57s$  configurations are mixed with  $4p^5nd$  configurations, whereas the  $4p^55s$  configuration can be considered pure.

Without this mixing one would qualitatively predict a strong decrease of the  $a_s$  parameter as a function of the principal quantum number  $n$ , because it contains a factor  $\langle 1/r^3 \rangle$  ( $r$  being the distance between the electron and the nucleus). Indeed, we find  $a_{6s}(^1P_1)/a_{5s} \ll 1$ . In contrast to this, the  $a_{6s}$  and  $a_{7s}$  parameters for the  $^3P_1$  states have roughly the same magnitude as  $a_{5s}$ . For both states strong interference by  $nd$  levels can be expected, particularly by the near-resonant  $4p^54d[{}^2P_{3/2}] J=1$  and  $4p^55d[{}^2P_{3/2}] J=1$  states, respectively.

Husson *et al.*<sup>17</sup> used the intermediate coupling wave functions for the Kr  $4p^5(5p+6p)$  configurations calculat-

ed by Aymar and Coulombe (private communication in Ref. 17) to calculate the matrix elements of the effective hyperfine Hamiltonian needed to obtain the  $A$  parameters of the  $4p^55p$  states. Their agreement with experimental results is much better than in an approach using pure configurations. Similar good agreement was obtained by Liberman for Ne  $2p^53s$ ,  $2p^54s$ , and  $2p^55s$  and Xe  $5p^5(6s+5d)$ .<sup>40,41</sup> A treatment of this kind is beyond the scope of the present paper. We are, however, considering additional experiments on the hyperfine structure of Kr  $4p^5nd$  levels, in conjunction with calculations on mixed configurations Kr  $4p^5(5s+6s+7s+4d+5d+6d)$ .

It should be noted that Aymar and Coulombe claim that the level designation for the  $6s[{}^2P_{3/2}] J=1$  level in Ref. 7 is incorrect and that the assignments for the  $6s[{}^2P_{3/2}] J=1$  and  $4d[{}^2P_{3/2}]$  levels should be interchanged.<sup>39</sup> This would obviously influence the parametrization of the  $A$  parameter [Eq. (6b)] for this level. However, Table VII does not seem to show any anomalous trends for the  $A$  parameter in going from the  $5s[{}^2P_{3/2}] J=1$  level through the  $6s[{}^2P_{3/2}] J=1$  level to the  $7s[{}^2P_{3/2}] J=1$  level.

It is important to see how these results influence our discussion of the  $B$  parameter. Our present conviction is that the conclusions concerning the coupling between the atomic core and the orbital electron are valid, since the analysis should not be affected very much by the inclusion of a small contribution to the quadrupole interaction by an  $nd$  orbital electron.

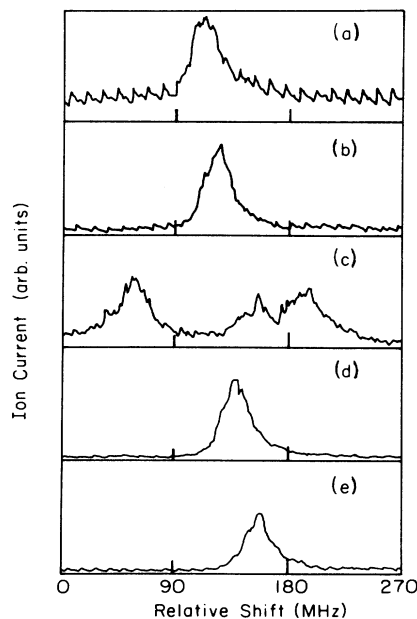


FIG. 3. Isotope shifts for the  $4p^6(1S_0) \rightarrow 7s[{}^2P_{3/2}] J=1$  transition: (a)  $^{80}\text{Kr}$ , (b)  $^{82}\text{Kr}$ , (c)  $^{83}\text{Kr}$ , (d)  $^{84}\text{Kr}$ , and (e)  $^{86}\text{Kr}$  ( $^{78}\text{Kr}$  is not shown because of a very poor signal-to-noise ratio). Isotope shifts are determined by measuring spectra of  $^{86}\text{Kr}$  and the isotope under consideration simultaneously. The periodic ripples in the spectra are the result of 60-Hz noise pick up.

TABLE VIII. Analysis of isotope shifts. The average ratio of the experimental isotope shifts and the calculated Bohr shifts for each  $4p^5ns$  configuration investigated (column 2) and the function  $R(M)$  for  $M=78,80,82,84$  [columns 3–6, see Eq. (10)]. Deviations from  $R(M)=1.00$  would indicate deviations from a pure mass effect.

State	$\left[ \frac{\Delta v_{\text{exp}}(M_1, 86)}{\Delta v_{\text{Bohr}}(M_1, 86)} \right]_{\text{av}}^a$	$R(78)$	$R(80)$	$R(82)$	$R(84)$
$5s' [{}^2P_{1/2}] J=1$	0.124	0.98(6)	1.03(8)	1.05(1)	0.92(19)
$6s' [{}^2P_{1/2}] J=1$	0.355	0.96(2)	1.01(3)	1.04(4)	0.99(6)
$6s [{}^2P_{3/2}] J=1$	0.265	1.00(3)	0.95(4)	1.01(5)	1.05(9)
$7s [{}^2P_{3/2}] J=1$	0.339	0.98(2)	0.99(3)	1.02(4)	1.01(7)

<sup>a</sup>Averaged over all pairs  $(M_1, 86)$  with  $M_1=78,80,82,84$ . For the  $5s [{}^2P_{3/2}] J=1$  a value of 0.103 was found.

### 3. Line intensities for $^{83}\text{Kr}$

For three of the five transitions studied, our observed hyperfine line strengths are in reasonable agreement with the theoretical predictions. The relative intensities are calculated to vary as  $2F+1$  for both unpolarized and linearly polarized light ( $J$  and  $F$  being the upper state quantum numbers). Only for the transitions to the  $6s [{}^2P_{3/2}] J=1$  and  $7s [{}^2P_{3/2}] J=1$  levels do we see a different pattern. In these cases the strength of the central component is only roughly half that of the neighboring ones ( $F=\frac{7}{2}$  and  $F=\frac{11}{2}$ ). At this point we have not come up with an explanation for this effect.

### C. Isotope shifts

Our isotope shift measurements were carried out by taking the spectra of  $^{86}\text{Kr}$  and the isotope under consideration simultaneously. The shifts are rather small, as is also observed for measurements in the visible and infrared spectral regions.<sup>10–12,23</sup> The spectra for the  $4p^6({}^1S_0) \rightarrow 7s [{}^2P_{3/2}] J=1$  transition are shown in Fig. 3, and the results for all transitions studied are listed in Table IV. The quality of our data for the transition to the  $5s [{}^2P_{3/2}] J=1$  level suffers from weak xuv power and, consequently, low signal at the conditions set for the necessary time-of-flight mass resolution. Thus we did not include these shifts in the table. The evaluation of the data indicates the  $5s [{}^2P_{3/2}] J=1$  level has slightly smaller shifts than the  $5s' [{}^2P_{1/2}] J=1$  level.

There are two effects which lead to the observation of isotope shifts. The first effect is due to the finite mass of the nucleus. This shift is usually written as a sum of two terms, the simple Bohr shift describing one-electron (hydrogenlike) atoms and a specific mass effect to account for electron correlations,<sup>10</sup>

$$\Delta v_{\text{mass}}(M_1, M_2) = \Delta v_{\text{Bohr}}(M_1, M_2) + \Delta v_{\text{SM}}(M_1, M_2), \quad (8a)$$

where

$$\Delta v_{\text{Bohr}}(M_1, M_2) = \frac{m_e(M_2 - M_1)}{M_1 M_2} E, \quad (8b)$$

and

$$\Delta v_{\text{SM}}(M_1, M_2) = K \Delta v_{\text{Bohr}}(M_1, M_2), \quad (8c)$$

with  $K$  being an electronic constant.

The second effect is a volume effect, found especially in heavy elements, due to the nonzero nuclear volume. It is expressed as the product of a state-dependent electronic factor  $E_v$  and an isotope-dependent nuclear volume factor  $V(M)$ ,<sup>42</sup>

$$\Delta v_{\text{volume}}(M_1, M_2) = E_v [V(M_1) - V(M_2)]. \quad (9)$$

In the first column of Table VIII the average ratio of the experimentally observed shift and the simple Bohr shift is printed for all states investigated. The ratios are significantly smaller than unity indicating a strong specific mass effect with a negative constant  $K$ . It is observed that as the energy of the excited state with respect to the ground state increases, the electron correlation decreases and there is a greater tendency to follow hydrogenlike behavior.

The present experiments are not conclusive about the presence of a volume effect. In columns 2–5 of Table VIII the ratios

$$R(M) = \frac{[\Delta v_{\text{expt}}(M, 86) / \Delta v_{\text{Bohr}}(M, 86)]}{[\Delta v_{\text{expt}}(M^*, 86) / \Delta v_{\text{Bohr}}(M^*, 86)]_{\text{av}}} \quad (10)$$

are given for all transitions investigated and all mass combinations  $(M, 86)$ . Here,  $\Delta v(M_1, M_2)$  is the isotope shift between masses  $M_1$  and  $M_2$ . If the observed isotope shifts can be explained in terms of a mass effect only, the value 1 will appear for all these ratios, whereas departures from a pure mass effect will show up as departures from unity. No conclusive departures from the value 1 are observed, indicating that within our experimental error all isotope shifts can be explained as mass effects.

As was also observed by Champeau and Keller<sup>13</sup> and by Jackson,<sup>15</sup> the  $^{83}\text{Kr}$  line centers do not necessarily lie on a smooth curve connecting the line centers for the other isotopes. The  $^{83}\text{Kr}$  offsets observed in the present experiments are listed in column 6 of Table IV and are significant only for the  $5s [{}^2P_{1/2}] J=1$  state.

#### D. Lifetime measurements

Lifetime measurements were performed for the 6s and 7s states by systematically delaying the ionizing laser with respect to the vuv pulse. The results are listed in Table V along with experimental and theoretical literature values for comparison. Our measurements should form a basis for improvements on the theoretical prediction which currently yield widely different and clearly erratic predictions.<sup>39,43</sup> Lifetimes for the 5s states were not

determined because they are significantly shorter than the resolutions of our laser pulses.<sup>36</sup>

#### ACKNOWLEDGMENTS

This work was supported by the Director, Office of Energy Research, Office of Basic Energy Sciences, Chemical Sciences Division of the U.S. Department of Energy under Contract No. DE-AC03-76SF00098.

\*Present address: Max-Planck-Institut für Extraterrestrische Physik, 8046 Garching bei Munchen, West Germany.

<sup>1</sup>H. Kopfermann and N. Wieth-Knudsen, *Z. Phys.* **85**, 353 (1933).

<sup>2</sup>H. Korsching, *Z. Phys.* **109**, 349 (1938).

<sup>3</sup>E. Rasmussen and V. Middelboe, *K. Dan. Vidensk. Selsk. Mat. Fys. Medd.* **30**, 3 (1955).

<sup>4</sup>F. Bayer-Helms, *Z. Phys.* **154**, 175 (1959).

<sup>5</sup>H. Kuiper and H. Friedburg, *Naturwissenschaften* **48-3**, 69 (1961).

<sup>6</sup>W. L. Faust and L. Y. Chow Chiu, *Phys. Rev.* **129**, 1214 (1963).

<sup>7</sup>V. Kaufman and C. J. Humphreys, *J. Opt. Soc. Am.* **59**, 1614 (1969).

<sup>8</sup>See references in Ref. 7.

<sup>9</sup>R. Czerwonka, P. Giacomo, and J. Hamon, *Metrologia* **6**, 74 (1970).

<sup>10</sup>C. Brechignac and S. Gerstenkorn, *J. Phys. B* **10**, 413 (1977).

<sup>11</sup>C. Brechignac, *J. Phys. B* **10**, 2105 (1977).

<sup>12</sup>D. A. Jackson, *J. Opt. Soc. Am.* **67**, 1638 (1977).

<sup>13</sup>R.-J. Champeau and J.-C. Keller, *J. Phys. B* **11**, 391 (1978).

<sup>14</sup>H. Gerhardt, T. Huhle, and J. Neukammer, *Opt. Commun.* **26**, 58 (1978).

<sup>15</sup>D. A. Jackson, *J. Opt. Soc. Am.* **69**, 503 (1979).

<sup>16</sup>X. Husson and J.-P. Grandin, *J. Phys. B* **12**, 3649 (1979).

<sup>17</sup>X. Husson, J.-P. Grandin, and H. Kucal, *J. Phys. B* **12**, 3883 (1979).

<sup>18</sup>J. Bokor, J. Zavelovich, and C. K. Rhodes, *Phys. Rev. A* **21**, 1453 (1980).

<sup>19</sup>D. A. Jackson, *J. Opt. Soc. Am.* **70**, 1139 (1980).

<sup>20</sup>C. Delsart, J.-C. Keller, and C. Thomas, *J. Phys. B* **14**, 3355 (1981).

<sup>21</sup>H. Abu Safia, J.-P. Grandin, and X. Husson, *J. Phys. B* **14**, 3363 (1981).

<sup>22</sup>T. J. Whittaker and B. A. Bushaw, *Proc. SPIE* **286**, 40 (1981).

<sup>23</sup>H. Gerhardt, F. Jeschonnek, W. Makat, E. Matthias, H. Rin-

neberg, F. Schneider, A. Timmermann, R. Wenz, and P. J. West, *Hyperfine Interact.* **9**, 175 (1981).

<sup>24</sup>T. J. Sears and A. R. W. McKellar, *Can. J. Phys.* **60**, 345 (1982).

<sup>25</sup>H. Abu Safia and X. Husson, *J. Phys. (Paris)* **45**, 863 (1984).

<sup>26</sup>C. R. Conf. Poids Mes. **6**, 85 (1960).

<sup>27</sup>*CRC Handbook of Chemistry and Physics*, 57th ed. (CRC, Boca Raton, 1976).

<sup>28</sup>B. Petersson, *Ark. Phys.* **27**, 317 (1964).

<sup>29</sup>E. Cromwell, T. Trickl, Y. T. Lee, and A. H. Kung (unpublished).

<sup>30</sup>S. Gerstenkorn and P. Luc, *Atlas du Spectra d'Absorption de la Molecule d'Iode (14800-20000 cm<sup>-1</sup>)* (Editions du Centre National de la Recherche Scientifique, Paris, 1978).

<sup>31</sup>S. Gerstenkorn and P. Luc, *Rev. Phys. Appl.* **14**, 791 (1979).

<sup>32</sup>C. E. Moore, *Atomic Energy Levels*, Natl. Bur. Stand. (U.S.) Circ. No. 467 (U.S. GPO, Washington, D.C., 1952), Vol. 2.

<sup>33</sup>H. Kopfermann, *Nuclear Moments* (Academic, New York, 1958).

<sup>34</sup>R. Aydin, *Phys. Lett.* **77A**, 419 (1980).

<sup>35</sup>J. B. Green, D. W. Bowman, and E. H. Hurlburt, *Phys. Rev.* **58**, 1094 (1940).

<sup>36</sup>E. Matthias, R. A. Rosenberg, E. D. Poliakoff, M. G. White, S.-T. Lee, and D. A. Shirley, *Chem. Phys. Lett.* **52**, 239 (1977).

<sup>37</sup>K. Goudsmit, *Phys. Rev.* **37**, 663 (1931).

<sup>38</sup>G. Breit and L. A. Wills, *Phys. Rev.* **44**, 470 (1933).

<sup>39</sup>M. Aymar and M. Coulombe, *At. Data Nucl. Data Tables* **21**, 537 (1978).

<sup>40</sup>S. Liberman, *Physica* **69**, 598 (1973).

<sup>41</sup>S. Liberman, *J. Phys. (Paris)* **30**, 53 (1969).

<sup>42</sup>W. H. King, *J. Opt. Soc. Am.* **53**, 638 (1969).

<sup>43</sup>P. F. Gruzdev and A. V. Loginov, *Opt. Spectrosc.* **38**, 611 (1975).